CHAPTER 9

Conclusions and Future Work

For the past two decades, GaN-based semiconductors have been researched extensively due to their applications in blue-UV regions of the electromagnetic spectrum. The work done thus far has witnessed improvements in crystal quality, where dislocation densities are reduced from 10^{14} to 10^{4} cm^{-2}. With the GaN-based materials and device technology being in the advanced stage, the studies presented in this thesis have resulted in advances in the characterization of the material and the fabrication of Schottky devices. Continued work and recommendations detailed at the end of this chapter will lead to further advancement and improvement in the blue/UV devices.

Various surface cleaning techniques and chemicals for the removal of contaminants from the GaN surface were investigated. Auger electron spectroscopy (AES) analysis was used to monitor the presence of surface contaminants while atomic force microscopy (AFM) was used to monitor surface roughness. AES analysis revealed that KOH was effective in removing carbon (C). When comparing the topographies of GaN surfaces cleaned in HCl, KOH and $(NH_4)_2S$ in aqueous solutions, it was found that surfaces treated in $(NH_4)_2S$ were most effectively cleaned with the lowest values of both C and O, RMS roughness and Ga/N ratio. This was as a result of $(NH_4)_2S$ preventing the re-oxidation of the GaN surface. The nearly complete removal of C and O was achieved by heating the samples in AES in ultra-high vacuum where contaminants on the GaN surface were removed by thermal desorption Using AES, it was found that carbon was purely a surface issue and, consequently, it was completely removed from the surface of GaN by thermal heating in a vacuum in AES.

GaN samples used in this study were grown on sapphire, requiring that both ohmic and Schottky contacts be fabricated on the same side of the material. This method of fabrication greatly reduces the active area of the Schottky barrier photodiode where UV light can be transmitted through to the semiconductor material. Thus the metals used must be transparent to UV radiation. A computer program was used to choose these metals, and it was found that

Ag, Ni and Au were most suitable, with modelled transparency of above 50% for a 10 nm thick layer. After extensive review, we chose to focus on Ni and Au, due to their high work function and barrier height. From literature, the transmission of Au was found to be higher than that of Ni with the same thickness, while that of annealed Ni/Au was 30% greater than that of Au and Ni. XRD analysis of GaN/Ni indicated that the transparent material on the surface is NiO, with SEM showing the surface mirror-like.

The effects of chemical cleaning on the electrical characteristics of Au Schottky contacts fabricated on n-GaN treated in HCl and $(NH_4)_2S$ have been investigated using current-voltage (I-V) and capacitance voltage (C-V) techniques. The reduction of surface oxide yielded a low series resistance. Current transport mechanisms of the diodes were dominated by thermionic emission with series resistance dominating higher voltages. $(NH_4)_2S$ was found to reduce barrier heights. It was found that the ideality factors of all diodes on GaN are above unity, requiring further studies of the interface states, which are believed to influence the values of both the ideality factors and Schottky barrier heights, which were found to have different values on the same diode at different positions. The best photodiodes were 0.25 mm in diameter, where the transport mechanism was almost purely themionic at lower voltages and series resistance at higher voltages.

Finally, the study was completed with the setting- up of an optoelectronic station for the evaluation of photonic devices. The setup consisted of a monochromator, an optical fibre and a deuterium light source, incorporated into the existing *I-V* station so that the measurements of dark and photocurrent could be carried out in the same system. GaN and AlGaN Schottky barrier photodiodes were fabricated using the Ti/Al/Ni/ Au ohmic contacts. Ni/Au was used to fabricate Schottky contacts. The photocurrent densities of GaN and AlGaN photodiodes recorded were 35.8 $\mu A/cm^2$ and 21.6 $\mu A/cm^2$ respectively. Device responsivity as high as 31.8 mA/W for GaN and 3.8 mA/W for AlGaN were recorded. The corresponding quantum efficiencies of the photodiodes were 11 % for GaN and 1.7 % for AlGaN respectively. The barrier heights of 0.67 eV and 1.09 were recorded, for GaN and AlGaN photodiodes. The commercial and fabricated AlGaN photodiodes have photocurrent density and responsivity maximum peaks occurring in the range of 270 - 280 nm.

The current-transport mechanisms of Schottky barrier diodes on GaN need to be explored in the same manner that Si has been researched. It is important to review the current-transport mechanisms on GaN, both experimentally and theoretically, in order to explain some anomalous behaviour such as the ideality factor far above unity, very high series resistance and barrier height inhomogeneity. The results of this thesis have shown that there is a problem with barrier height values and ideality factors reported in literature on new materials like GaN and AlGaN. The values are often scattered and an inconsistency is evident in the methods of preparation, growth of samples and metals used. Although Si has been used to lay a foundation for all semiconductor materials, it does not necessarily mean that the results concerning Si can be assumed for other materials. The optoelectronic station could be improved by extending its use to visible and infrared regions of electromagnetic radiation so that the research spreads out to all photonic devices.

From this thesis, several issues in the fabrication and characterization of Al(GaN) remain unresolved and deserve further investigations. Future work should focus on:

- The improve heterostructure should have AlN layer thickness reduced to some few nanometres so that series resistance should be lowered.
- Establishing wet etch rates for (Al)GaN heterostructures so that ohmic contacts can be fabricated onto the GaN layer.
- Fabrication of (Al)GaN ohmic contacts.
- Determination of more parameters for the evaluation of UV photodiodes:
    - Detectivity
    - Noise equivalent power and
    - Response speed

List of Publications

1. **M. Diale**, C. Challens, E. C. Zingu, Applied Physics Letters **62** (1993) p943, **Cobalt self diffusion during cobalt silicide formation.**
2. T. L. Alford, D. Adams, **M. Diale**, J. Li, S. A. Rafalski, R. L. Spreitzer, S. Q. Hong, S. W. Russel, N. D. Theodore, and J. W. Mayer, In: D. P. Fayreau, Y. Shacham-Diamand and Y. Horiike, Editors, MRS Pittsburg, PA(1993) p49, **Advanced metallization of USLI Applications.**
3. T.L. Alford, E.J. Jaquez, N.D. Theodore, S.W. Russell, **M. Diale**, D. Adams and S. Anders, J. Appl. Phys **79** (1996), p2074, **Influence of interfacial copper on the room temperature oxidation of silicon.**
4. H. W. Kunert, D. J. Brink, M. Hayes, J. Malherbe, L. Prinsloo, J. Barnas, AGJ Machatine, and **M. Diale**, Physica Status Solidi C 1(2) (2004) p223,**Optical characterization of GaN doping superlattices: As grown, hydrogen implanted, and annealed.**
5. **M. Diale,** F. D. Auret, N. G. van der Berg, R. Q. Odendaal, W. D. Roos, Applied Surface Science 246 (2005) p279, **Analysis of GaN Cleaning procedures.**
6. **M. Diale,** F. D. Auret, N. G. van der Berg, R. Q. Odendaal, W. D. Roos, Surface and Interface Analysis 37 (2005) p115, **Study of Carbon behaviour on GaN surface in ultra-high vacuum (UHV).**
7. G. H. Kassier, M. Hayes, F. D. Auret, **M. Diale**, B. G. Svensson, Physica Status Solidi C 1(5) (2008) p569, **Hall effects study of donors and acceptors in different types of bulk ZnO modified by annealing and hydrogen implantation.**
8. W. Mtangi, F. D. Auret, C. Nyamhere, P. J. Janse van Rensburg, **M. Diale**, A. Chawanda, Physica B **404** (2009) p1092, **Analysis of temperature dependent I-V measurements on Pd/ZnO Schottky barrier diodes and the determination of the Richardson constant.**
9. **M. Diale** and F. D. Auret, **Effects of chemical treatment on Au-GaN Schottky barrier diodes**, accepted by Physica B, 2009.
10. W. Mtangi, F. D. Auret, C. Nyamhere, P. J. Janse van Rensburg, **M. Diale**, J. M. Nel and W. E. Meyer, Physica B **404** (2009) p4402, **The dependence of**

barrier height on temperature for Pd Schottky contacts on ZnO.

11. L. van Schalkwyk, **M. Diale**, W. E. Meyer and F. D. Auret, SMEOS 2009, South African Journal of Science, 2009, **Optoelectronic study of Schottky photodiodes on AlGaN.**
12. A. Chawanda, C. Nyamhere, F. D. Auret, W. Mtangi, T Hlatswayo, **M. Diale**, and J. M. Nel, Physica B **404** (2009) p4482, **Thermal stability study of palladium and cobalt Schottky contacts on n-Ge(100) and defects introduced during contacts fabrication and anneal.**
13. A. Chawanda, C. Nyamhere, F. D. Auret, W. Mtangi **M. Diale**, J. M. Nel, Physica Status Solidi C 1-4 (2010), **Comparison of metal Schottky contacts on n-Ge (100) at different annealing temprreratures.**
14. A. Chawanda, C. Nyamhere, F. D. Auret, W. Mtangi **M. Diale**, J. M. Nel, Journal of Alloys and Compounds 491 (2010), **Thermal annealing behaviour of platinum, nickel and titanium Schottky barrier diodes on n-Ge(100)**.

UNIVERSITEIT VAN PRETORIA
UNIVERSITY OF PRETORIA
YUNIBESITHI YA PRETORIA

ELSEVIER

Available online at www.sciencedirect.com

SCIENCE DIRECT®

Applied Surface Science 246 (2005) 279–289

applied surface science

www.elsevier.com/locate/apsusc

Analysis of GaN cleaning procedures

M. Diale[a,*], F.D. Auret[a], N.G. van der Berg[a], R.Q. Odendaal[a], W.D. Roos[b]

[a]*University of Pretoria, Department of Physics, Lynnwood Road, Pretoria 0001, South Africa*
[b]*University of Free State, Bloemfontein, South Africa*

Received 5 August 2004; accepted 12 November 2004
Available online 30 December 2004

Abstract

In this study, various surface cleaning techniques for the removal of contaminants from GaN were investigated. Auger electron spectroscopy (AES) analysis was used to monitor the presence of surface contaminants and atomic force microscopy (AFM) was used to monitor surface roughness. AES analysis showed that KOH was effective in removing carbon (C). Comparing the topographies of GaN surfaces cleaned in HCl, KOH and $(NH_4)_2S$ in aqueous solutions; it has been found that surfaces cleaned in $(NH_4)_2S$ is the best cleaned, have the lowest values of both C and O, RMS roughness and Ga/N ratio. The nearly complete removal of C and O were achieved by heating the samples in AES in vacuum.

PACS: 73.61

Keywords: Morphology; Wet chemical; Cleaning; GaN

1. Introduction

A number of groups have investigated GaN cleaning procedures for device fabrication [1–5]. The importance of properly cleaned surfaces for ohmic and Schottky contacts deposition is well known [4,5]. There is currently no standard method of preparing the GaN substrate prior to metallization. Preparation methods differ from one laboratory to the other. Wet and dry etching methods are widely used in surface preparation for removal of surface contaminants. In addition, the morphology of the surface of the substrate prior to metallization has an influence on the continuity of the ultra-thin metals used in fabrication of Schottky barrier diodes for UV detection. Wet and dry cleaning of substrates using chemicals have been used on GaN prior to metallization. Dry cleaning methods are known for introducing damage to the surface, usually making the material electrically unsuitable [6]. Various surface analytical techniques such as Auger electron spectroscopy (AES), X-ray photoelectron spectroscopy (XPS), low energy electron diffraction (LEED), and secondary ion mass spectroscopy (SIMS) have been used to identify the

* Corresponding author. Tel.: +27 12 420 4418;
fax: +27 12 362 5288.
E-mail address: mdiale@postino.up.ac.za (M. Diale).

0169-4332/$ – see front matter
doi:10.1016/j.apsusc.2004.11.024

surface contaminants, oxides, metal particulate and reconstruction. Atomic force microscopy (AFM) has been used to monitor the surface cleanliness as a function of topography [7,8].

The work done by Smith et al. in cleaning GaN has shown that the choice of cleaning chemical is of utmost importance [1]. In their work, they used AES to compare HCl- and HF-based solutions in methanol and in water, to remove contaminants on the GaN surface. The use of UV/O_3 treatment was also done. All the chemical cleaning was followed by thermal desorption at temperatures of up to 800 °C to completely produce a contamination-free surface. From their results, it was observed that dissolving HCl in deionised water (DI) resulted in cleaner surfaces as compared to dissolving in methanol. HF results showed that C (carbon) and O (oxygen) residues were lower in HF:DI solution than in HF:methanol solution. These results were influenced by the physiosorption of methanol, thus increasing C content on the surface of GaN. Comparing HCl:DI and HF:DI, it was found that HF-based solution was more effective in removing both C and O on the surface. A further observation was the presence of Cl on the surface after treatment with HCl-based solution and UV/O_3 increased the surface oxide while decreasing the C. The best cleaning method according to Smith et al. is the final step, in which HF was diluted in deionised water as it removed most of the C, O and Cl without leaving any traces of F on the surface. The thermal desorption results showed further reduction of C and O as the temperature is gradually increased up to 800 °C, beyond which the decomposition of GaN was observed.

Further work done by King et al. using XPS and AES, on both AlN and GaN showed that different chemicals may be used to yield atomically clean surfaces [2]. They used HCl, HF, NH_4F, HNO_3, H_2SO_4, H_3PO_4, H_2O_2, NH_4OH, NaOH, KOH, RCA SC1 and SC2 (1:1:5 NH_3OH:H_2O_2:H_2O at 85 °C and 1:1:5 HCl:H_2O_2:H_2O at 85 °C) and TCE, acetone, methanol and UV/O_3 treatment. Thermal desorption was done in an integrated UHV system at temperatures of up to 1100 °C. As in the previous work by King et al., UV/O_3 was found to be effective in removing C and simultaneously increasing O on the surface. In addition to reducing the C peak, the exposure to UV/O_3 moved the C peak to higher energies, consistent with oxidation of C species on the surface of GaN. It was observed that increasing ozone concentration further reduced C on the surface though it was not completely removed. Further observations of the UV/O_3 exposed surface, showed an increase in the rate of oxidation of GaN surface, as seen in complete disappearance of N KLL and N1s peaks. The observed oxides were found to be in the form of Ga_2O_3 and N–O at binding energies 20.8 and 398.2 eV, respectively.

The use of HCl, NH_4OH and HF solutions were found to remove the oxides effectively. A 1:1 HCl:DI solution was found to produce the lowest C/N ratio with a disadvantage of Cl addition to the surface. The O coverage on the HCl sample was found to be inversely proportional to Cl detected on the surface. According to their results, the fact that the N–Cl bond strength is less than that of Ga–Cl gave an explanation why there is Cl residue on GaN surface. The results of using H_2SO_4 and H_3PO_4 were observed residues of SO_4 and PO_4 on the surfaces of GaN, increasing surface oxide coverage after these treatments. The 1:10 HF-based cleaning solutions were found to increase the O/N ratio with no detection of F on the surface. Stoichiometric GaN surface was produced after annealing the surfaces at 700–800 °C in NH_3. Using thermal desorption, it was found that HCl cleaned samples showed complete desorption of all contaminant species on the surface after 950 °C. AFM was used to investigate the surface roughness of the cleaned surfaces. All samples had surface RMS roughness comparable with the as-grown material, while H_3PO_4 resulted in increased surface roughness from as low as 20 Å to as high as 200 Å. On the GaN surface, the RCA SC1 and SC2 reduced the UV/O_3 oxides, though SC2 left more C on the surface relative to SC1.

Lee et al. investigated several methods of cleaning GaN [3]. The methods included different wet chemical procedures, as well as in situ cleaning in AES at elevated temperatures. The wet chemical methods consisted of acetone, methanol, HF or HCl and UV/O_3 treatments. Thermal cleaning was done in N_2 and H_2/N_2 plasma. UV/O_3 increased the O on the surface while decreasing the C peak. Using AES, it was observed that the surface of the as-grown (as-received) sample contained about 12% C and 13% O and that the Ga/N ratio was 1.08. Applying photoresist and stripping it with acetone reduced the O content slightly, and increased the carbon content to 30%. Treatment in HCl further reduced the O concentration to 7% and the C content to almost the same level as of the as-grown sample. The HCl treatment also left Cl contamination on the surface. Using thermal cleaning after various chemical treatments reduced the C and O surface content to below the detection limit of AES. AFM results showed insignificant change in surface roughness after all the wet chemical cleaning on GaN surface.

The work by Pelto et al. in pre-metallization treatment of GaN for ohmic contacts fabrication showed that the surface cleaning recipes depends on what device is being fabricated [4]. The following etch recipes were used: H_2SO_4:H_3PO_4:DI (1:1:2), HCl:DI (1:2), HNO_3:HCl (1:3), and NH_4OH:DI (1:10). The ohmic contacts' behaviour depended on the etch recipe used, and the expected outcomes. On the other hand, Machuca et al. used a simple cleaning method focusing on the optimization of electron emitters with wide bandgap [5]. Using H_2SO_4:H_2O_2 (4:1) to reduce contaminants on GaN surfaces followed by annealing in vacuum at 700 °C, they showed that after chemical clean, the vacuum anneal was best for thermal desorption of C and O than annealing in NH_3. Both these authors do not comment on any remaining surface contaminants on GaN and their effects on electrical properties of the devices made.

Thermal desorption in the vacuum has been recommended as a final step in most cleaning procedures. In particular, thermal desorption done in vacuum have shown that all the surface contaminants can be reduced to less than the AES detection limit. In the above works done, it can be summarized that thermal desorption of contaminants on GaN is independent of what has been used chemically prior to heating. Heating the material to a temperature range from 800 to 1000 °C has shown complete removal of C all contaminants on GaN surface [1–3].

The above review shows that there is still a gap in GaN cleaning procedures used prior to metallization. There is need to test the effects of chemical cleaning procedures by evaluating electrical characteristics of devices. In this work, we have investigated chemical cleaning of GaN surfaces and evaluating the results with AFM and AES. A variety of wet chemistries for O and C removal were investigated. We particularly report on the effects of HCl, KOH and $(NH_4)_2S$ on GaN surfaces. In addition, we give thermal cleaning results.

2. Experimental

n-GaN samples of orientation (1 0 0 0) and unintentional doping of $1.6 \times 10^{16}\ cm^{-3}$ were obtained from AIXTRON, grown by metal organic chemical vapor deposition (MOCVD) on sapphire (Al_2O_3) substrate. The thickness of the GaN layer was 1 μm. The cleaning methods used are summarized in Table 1. All samples were finally blown dry with compressed nitrogen gas of ultra-high pure quality. Only analytical grade quality chemicals were used and all water rinses were done in deionised water ($\rho > 18\ M\Omega\ cm$). All samples used in this study were cut from the same wafer as GaN growth techniques are not yet well established as compared to other semiconductors. Ultrasonic rinse was employed to ensure the removal of all loose debris on the surface. All cleaning

Table 1
Outline of cleaning procedures

Number	Procedure
Degrease	Boil in trichloroethelyne for 3 min Boil in isopropanol for 3 min Three rinses in DI for 20 s each Blow dry with N_2
Aqua regia (AR)	Degrease Boil in HCl:HNO_3 = 3:1 for 8–10 min Three rinses in DI for 20 s each Blow dry in N_2
HCl	Degrease Aqua regia HCl:H_2O = 1:1 dip for 60 s Two rinses in DI for 20 s each Blow dry with N_2
KOH	Degrease Aqua regia 1 mol KOH boil for 3 min Three rinses in DI for 60 s each Blow dry with N_2
$(NH_4)_2S$	Degrease Aqua regia $(NH_4)_2S$ for 1 min Three rinses in DI for 60 s each. Blow dry with N_2

equipments used were made of pure quarts glass and Teflon. Samples were loaded into the AES immediately after wet chemical cleaning.

Thermal cleaning was done by mounting the degreased sample onto a heater block and loaded into the AES, PHI model 549. The analysis was carried out from room temperature of 23 °C, continually monitoring the surface up to a temperature of 1100 °C. The heating process was stopped at this stage to avoid any decomposition of GaN into the AES system.

The scanning probe microscope used in this study was a commercial instrument model, Topometrix 2000 Discoverer. The topographical features of GaN crystals were studied by means of AFM in contact mode. The 130 and 7 μm scanner and standard Topometrix Si_2N_3 tips were applied. All scans were applied under ambient conditions. Several images were taken at different positions on the sample to gain better understanding of the surface topography. The same scan parameters (set point, proportional gain, integral gain and derivative gain) were used; however, in each scan, optimizations were performed. The topography of the surfaces was analysed from obtained images, using the surface roughness parameters: the root mean square (RMS) roughness, maximum peak height from the mean line, R_p; the maximum peak to valley height in the profile, R_t.

The AES study was carried out on Physical Electronics Model 545 Spectrometer, using a cylindrical mirror analyzer with 5 keV electron beam incident on samples mounted on a sample holder of which the angle with the electron beam is 30°. The percentage surface concentration was calculated from the peak-to-peak heights and relative sensitivity factors for different elements.

3. Results and discussion

3.1. AFM

AFM images from randomly selected 5 μm × 5 μm areas of degrease to $(NH_4)_2S$ cleaned surfaces are presented in Figs. 1–3. The images, together with corresponding line profiles, indicate difference in topography of investigated GaN surfaces after every cleaning method. The as-grown surface has been degreased to deal with packaging contaminants.

The as-grown surface has needle-shaped protrusion as shown in Fig. 1(a). Using R_t, we compared the difference in features, ranging from protrusions to craters. From R_t measurements, the average height of the protrusions on the surface of the degreased samples was found to be 20.05 nm, as shown in Table 2. The second surface, represented in Fig. 1(b), was cleaned in aqua regia and shows a disappearance of the protrusions and the emergence of craters, which are hexagonal in shape, with R_t value decreasing to 2.5 nm. This observation implies that the chemicals used thus far, were able to act on the protrusions on the as degreased surface, characterizing GaN by showing hexagonal structure of the crystal.

The next step is etching the surface in HCl, and it is observed that protrusions are disappearing from the surface and craters are increasing, as shown in Fig. 2(a). These craters are either isolated or joint to form a bigger crater on the surface and the value of R_t increasing to 13.36 nm, indicating deeper craters as protrusions are removed. The surface protrusions seem to have changed shape, from needles to rounded protrusions. The use of KOH on the surface, as shown in Fig. 2(b), shows that the protrusions appeared to be white and flat-shaped. In Fig. 3, the surfaces of the samples cleaned in $(NH_4)_2S$ are shown. The protrusions on this surface are quite similar to the ones on the KOH etched surface. A two-dimensional (2D) image of the sample cleaned in $(NH_4)_2S$ is shown in Fig. 3, confirming that the observed protrusions on the surface are part of the crystal.

The density of craters on each of the three last cleaning processes is similar, particularly for the HCl and KOH surfaces at approximately $6.2 \times 10^8\ cm^{-2}$. The $(NH_4)_2S$ surface has a little lower density of craters at approximately $5.3 \times 10^8\ cm^{-2}$. The approximated density of craters is similar to the dislocation density of the GaN used in this experiment, which is approximated to be 10^7 to $10^8\ cm^{-2}$. Comparing the cleaning procedures, it was found that GaN was etched along the threading dislocation. Threading dislocations have been found to be dominant defects in GaN from TEM studies. In addition, the observed decrease in the density of the craters shows that a new surface has appeared. It has been observed from TEM studies that threading dislocation decrease gradually away from the interface [9].

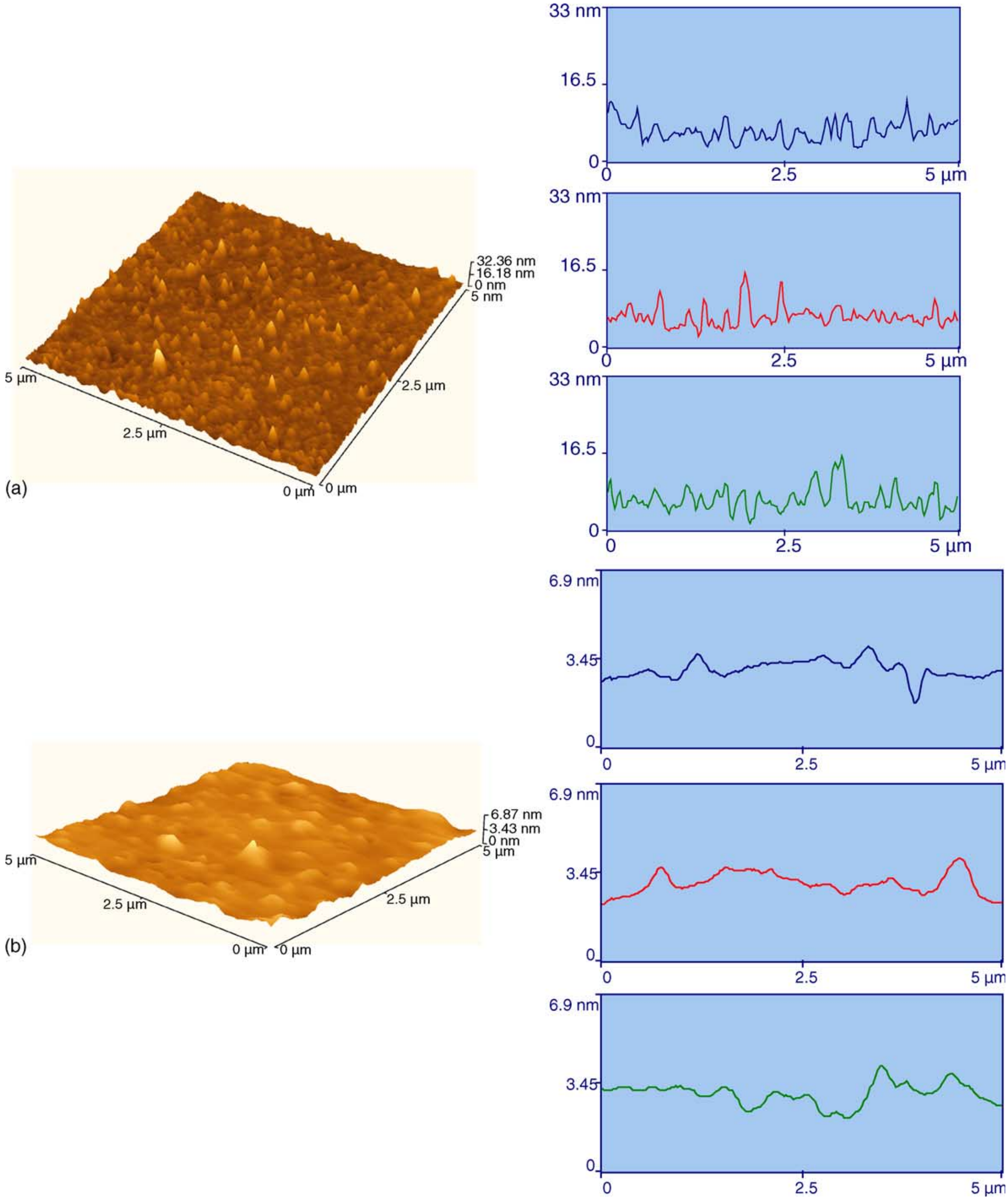

Fig. 1. AFM images taken from selected 5 µm × 5 µm areas of GaN surfaces cleaned by (a) degrease and (b) aqua regia, and the corresponding line profiles.

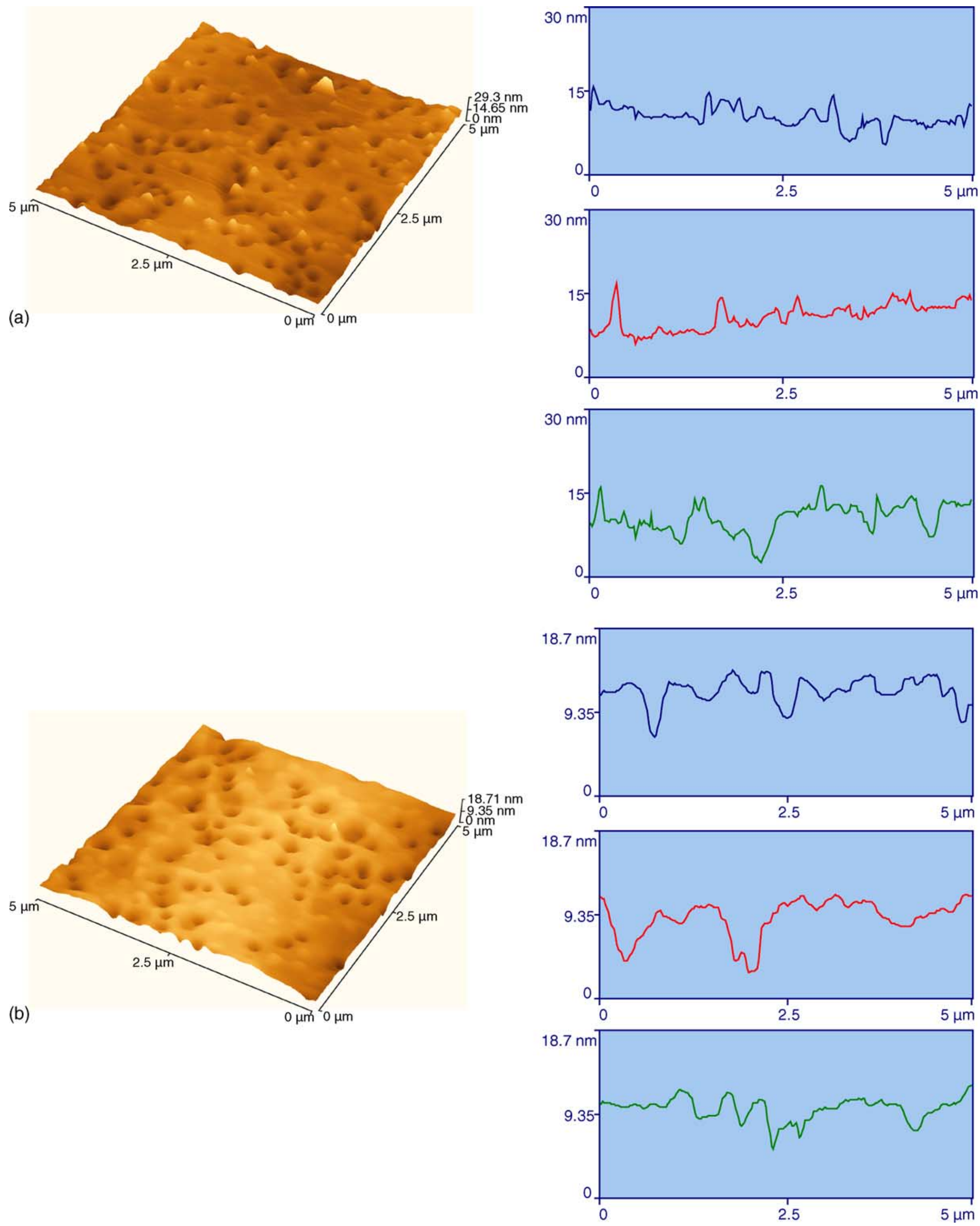

Fig. 2. AFM images taken from selected 5 µm × 5 µm areas of GaN surfaces etched as indicated and the corresponding line profiles.

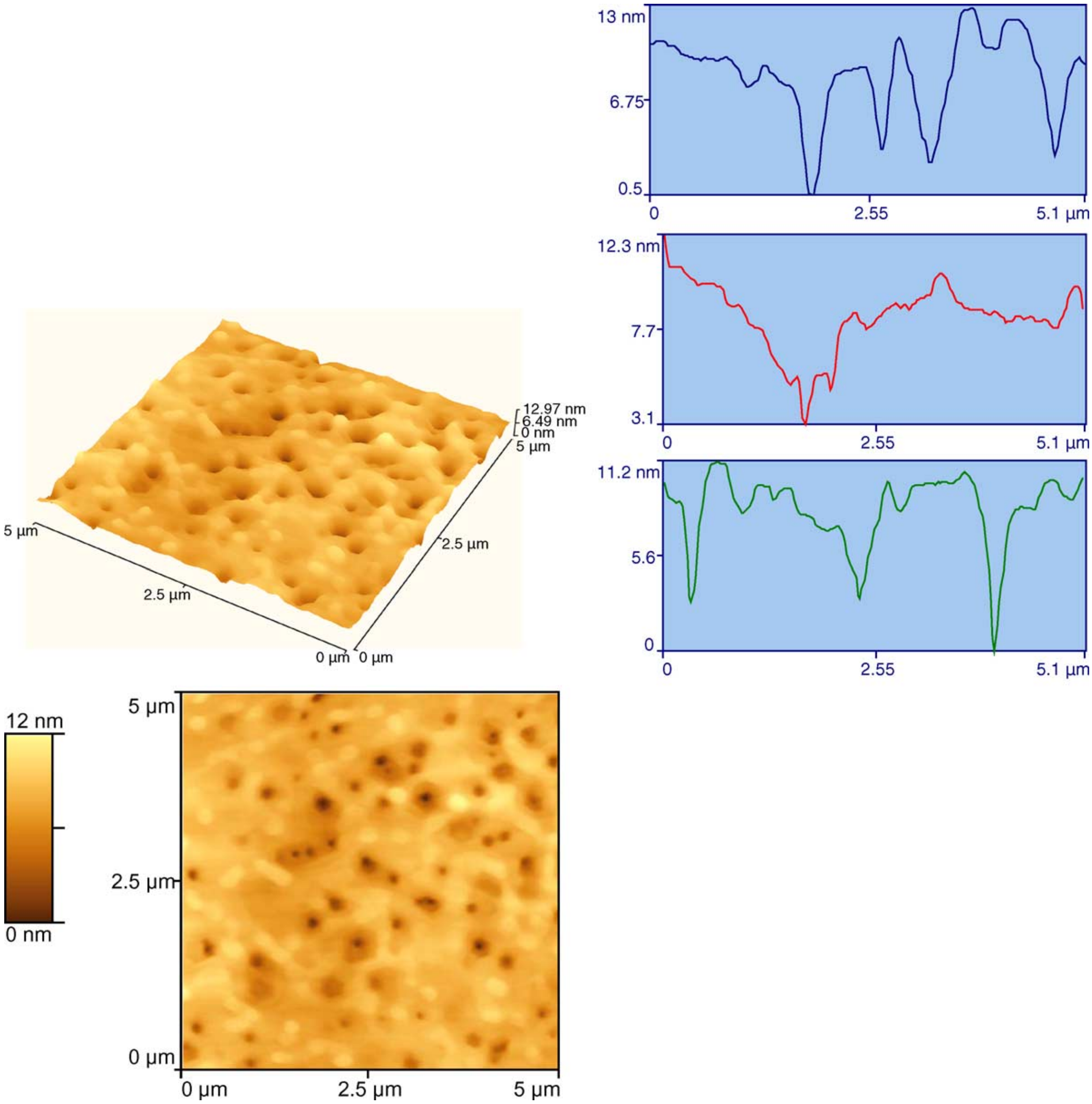

Fig. 3. AFM images taken from selected 5 µm × 5 µm areas of GaN surfaces etched as in $(NH_4)_2S$, the corresponding flat image and line profiles.

KOH has been used to characterize defects in GaN, and the defects density was found to be 2×10^9 cm^{-2}. Different values of defect densities have been recorded as 3×10^7 and 4×10^7 cm^{-2} on N-face, and 1×10^7 and 5×10^5 cm^{-2} on Ga-face. The understanding of the mechanisms for the formation thereof, will lead to the reduction of these defects [10].

Using line profiles, statistical parameters were deduced from the AFM for each of the cleaning procedures and are shown in Table 2 [11]. From the analysis of these data, the morphologies of differently cleaned surfaces differ from one cleaning method to the other. The value of R_t changed from 20.5 nm for degreased sample to 2.5 nm after aqua regia treated, implying a removal of surface protrusions. The last three etch processes also differ in the value of R_t, indicating how one chemical is able to etch the GaN surface. KOH and $(NH_4)_2S$ each were able to produce

Table 2
Statistical characterization of GaN single crystal surfaces by AFM

Cleaning procedures	Maximum topography variation (R_t, nm)	Parameter		
		Mean topography variation (R_p, nm)	RMS surface roughness (nm)	Roughness factor
Degrease	20.05	11.27	1.74	1.006
Aqua regia	2.5	1.55	0.4	1.060
HCl	13.36	7.0	2.02	1.010
KOH	11.03	4.03	2.1	1.077
$(NH_4)_2S$	8.74	2.74	1.2	1.098

new surfaces as compared to HCl, which was not able to produce a new surface. The other parameters, R_p, RMS roughness and the roughness factor all confirm the R_t values. The highest RMS roughness is from the KOH etched surface and the lowest is from the aqua regia cleaned surface. Furthermore, using RMS roughness parameter, we have compared the stoichiometries on each of the cleaned surfaces, and stoichiometry and RMS roughness are compared as shown in Fig. 5.

3.2. AES

AES was used to analyze the surface contaminants and the results are shown in Fig. 4. The effect of the cleaning procedure is seen in the reduction of O and C peaks. In addition to reducing C and O peaks, HCl in aqua regia and $(NH_4)_2S$, respectively, added Cl and S to the surface. The atomic percentage of surface elements present on every surface after wet chemical cleaning procedures was calculated from the relative sensitivity factors. These contaminants may be of advantage to the metal contact formation on the GaN surface as bonding with Au may be enhanced and adhesion improved. Furthermore the use of sulfurants, alkenoids and halogens has proved to enhance adhesion of metals such as Au, Ag, Pt, Pd and Ni to semiconductor surfaces [12,13].

Comparing the AES surface scans of HCl and $(NH_4)_2S$, it is found that using HCl on the GaN surface reduced the O peak, added Cl, and the use of $(NH_4)_2S$ prevents re-oxidation of the surface, adding insignificant amount of S, and reducing the Cl contaminant. This result further confirms the importance of using

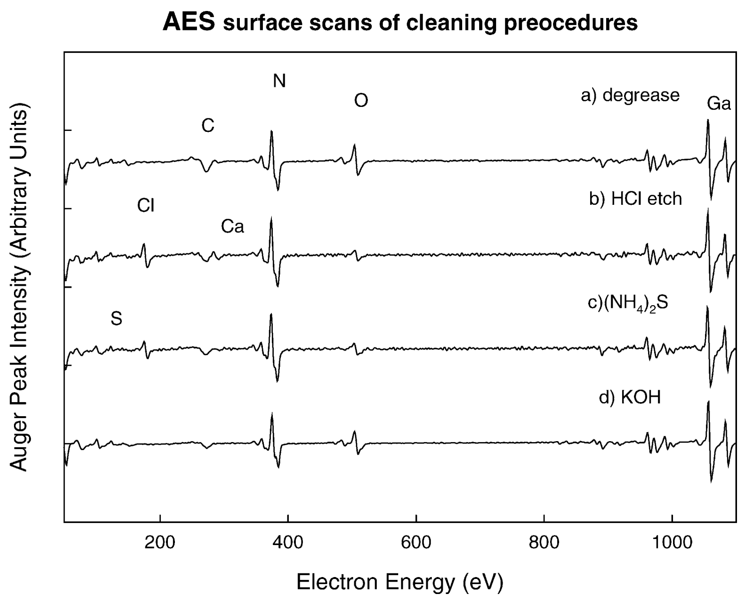

Fig. 4. AES surface scans of GaN surfaces cleaned as indicated.

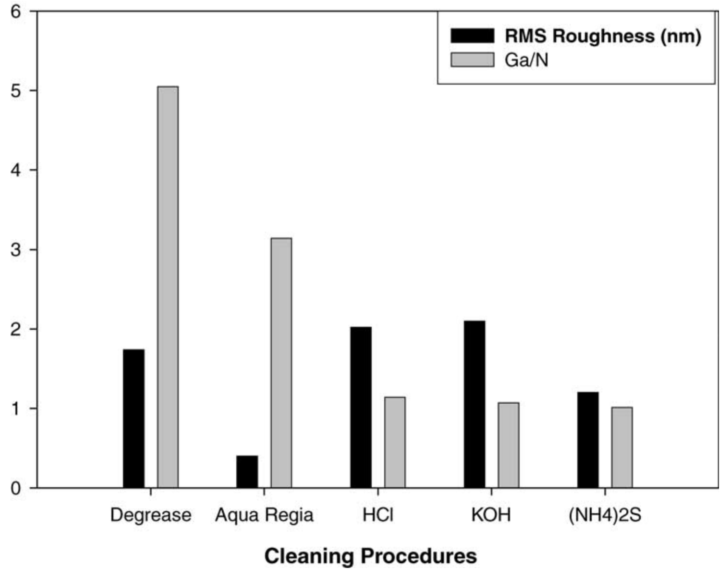

Fig. 5. Graph of root mean square (RMS) surface roughness and Ga/N ratio from AES elemental surface concentrations. Ga/N ratio close to 1 is stoichiometric.

$(NH_4)_2S$ as a chemical that prevents re-oxidation of surfaces. KOH removed all the Cl from the surface, and reduced the C significantly.

There had been reports of improved electrical characteristics of metals/GaN contacts after treatments in HF, HCl, and NaOH. Miller et al. has reported the reduction of reverse bias leakage current in GaN Schottky diodes after treatment in NaOH. The high concentration of OH-ion on the GaN surface is attributed to the reduction of reverse bias leakage in their Schottky contacts [14]. In another report, Lin and Lee has reported the reduction of surface states on InGaN using $(NH_4)_2S$ [15]. Electrically, $(NH_4)_2S$ was reported to reduce the Schottky barrier height. In particular, it was reported that Ga–O, In–O and C–O bonds were removed from the InGaN surface after $(NH_4)_2S$ treatment. Furthermore, repeated exposure of the surface that has a Cl peak to the electron beam in the AES system has resulted in desorption of the surface contaminants, and consequently, complete removal of the Cl peak.

To further analyse the cleaned surfaces, the ratio of Ga/N, and RMS surface roughness are plotted as a function of cleaning method, as shown in Fig. 5. There is a relationship between the RMS surface roughness and the contaminants on the surfaces, which consequently affects the Ga/N ratio. The as-grown surface shows a very high surface roughness and Ga/N ratio and the cleanest surface shows lowest surface roughness and Ga/N ratio. Therefore as the surface is cleaned, the surface roughness reduces as the Ga/N ratio improves, implying that the chemicals used has etch GaN surface to remove contaminants. The RMS surface roughness of KOH etched surface, differ from the as-grown surface by about 0.4 nm. Different wet chemicals used previously in removing contaminants on GaN have shown no effect on the surface roughness of the material [2,3]. The work done previously to etch and remove surface GaN to form etch steps were not achieved by using HCl and KOH [16]. Ultraviolet light illumination and addition of ions were used to etch GaN successfully in KOH [17].

Previous results have recommended the use of thermal desorption after every chemical clean, to completely remove surface contaminants [1–3]. In this work, we have found that thermal cleaning of the degreased GaN surface resulted in almost complete removal of surface contaminants. Fig. 6 is a typical temperature profile of a sample cleaned in UHV under high temperatures. This profile may be divided into two regions: region 1 from 23 to 500 °C and region II from 500 to 1010 °C. In region I, the carbon peak first

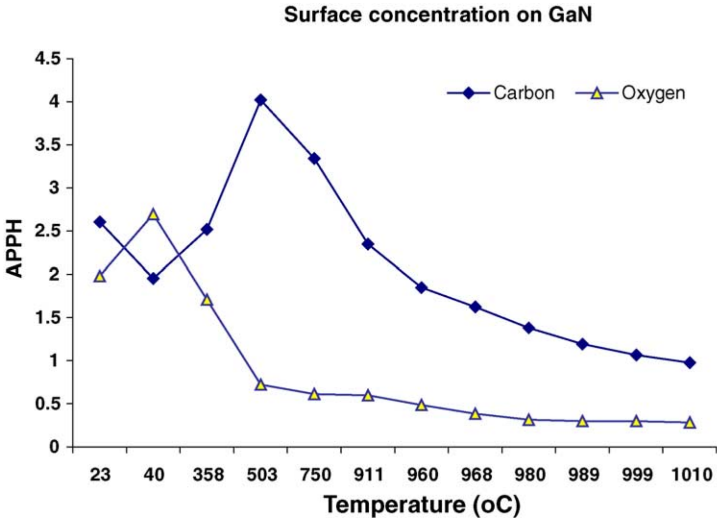

Fig. 6. Surface concentration profiles of O and C on GaN surface during thermal anneal in the AES.

decreases and then increases as temperature increases. In region II, the carbon coverage on the surface of GaN decreases until it drops to below AES detection limit, where average peak-to-peak height is less than 1.5. In the case of oxygen, the surface coverage starts increasing and quickly decreases sharply until the temperature of about 500 °C. At this temperature, all oxides are removed from the surface according to AES sensitivity, in which average peak-to-peak height is less than 0.5. The increase in O from 23 to 50 °C may be attributed to the removal of common surface water that had been covering the surface prior to thermal heating. This water is very sticky and is usually removed at temperatures above 220 °C. On the other hand, the increase in C may be due to segregation from the bulk, which needs further study to confirm.

4. Conclusions

In conclusion, the effectiveness of wet chemical cleaning of GaN with different solutions, have been characterized by AFM and AES. AFM results have shown that GaN surface roughness is affected by the cleaning method used on the surface. Surface defects were characterized by different etch chemicals, with $(NH_4)_2S$ producing a defect-free interface. AES has shown the contaminant as C and O and that using compounds with Cl and S, will leave Cl and S on the surface. This result has given sufficient information on removal of surface contamination; stoichiometry; surface roughness and chemical etch. Using $(NH_4)_2S$ prevented re-oxidation of the surface, and further removes Cl from the surface of the GaN. KOH effectively removes the C on the surface. The effects of S and Cl on the surface may enhance adhesion of metals to GaN surface, thus improving device quality.

Further work is necessary in finding the effects of different cleaning procedures on the optical properties of the material and electrical properties of devices.

Acknowledgements

The National Research Foundation, the University of Pretoria and the University of Free State funded the project.

References

[1] L.L. Smith, S.W. King, R.J. Nemanich, R.F. Davis, J. Electron. Mater. 25 (1996) 805.
[2] S.W. King, J.P. Barnak, M.D. Bremster, K.M. Tracey, C. Ronning, R.F. Davis, R.J. Nemanich, J. Appl. Phys. 84 (1998) 5248.
[3] K.N. Lee, S.M. Donovan, B. Gila, M. Overberg, J.D. Mackenzie, C.R. Abernathy, R.G. Wilson, J. Electro. Chem. Soc. 147 (2000) 3087.

[4] C.M. Pelto, Y.A. Chang, Y. Chen, R.S. Williams, Solid State Electron. 45 (2001) 1597.
[5] F. Machuca, Z. Liu, Y. Sun, P. Pianetta, W.E. Spicer, R.F. Pease, J. Vac. Sci. Technol. A 20 (2002) 1784.
[6] R.J. Shul, G.A. Vawter, C.G. Willison, J.W. Lee, S.J. Pearton, C.R. Abernathy, Solid Stat. Electron. 42 (1998) 2259.
[7] J.M. Nel, C.M. Demanet, K.T. Hillie, F.D. Auret, H.L. Gaiger, Appl. Surf. Sci. 134 (1998) 22.
[8] P.N.K. Deenapanray, F.D. Auret, G. Myburg, K.T. Hillie, C.M. Demanet, Surf. Interf. Anal. 26 (1998) 748.
[9] J. Jasinki, W. Swider, Z. Liliental-Werber, P. Visconti, K.M. Jones, M.A. Reshchikov, F. Yun, H. Morkoc, S.S. Park, K.Y. Lee, Appl. Phys. Lett. 78 (2001) 2297.
[10] H. Morkoc, Mat. Sci. Eng. R33 (2001) 135.
[11] D. Zymierska, J. Auleytner, T. Kobiela, R. Dus, Phys. Solid State (a) 180 (2000) 479.
[12] J. Wang, B. Zeng, C. Fang, X. Zhou, J. Electroanal. Chem. 484 (2000) 88.
[13] I. Shalish, Y. Shapira, L. Burstein, J. Salzan, J. Appl. Phys. 89 (2001) 390.
[14] E.J. Miller, D.M. Schaadt, E.T. Yu, P. Walterit, C. Poblenz, J.S. Speck, Appl. Phys. Lett. 82 (2003) 1293.
[15] Y.-J. Lin, C.-T. Lee, J. Vac. Sci. Technol. B 9 (2001) 1734.
[16] C.B. Vartuli, S.J. Pearton, C.R. Abernathy, J.D. Mackenzie, F. Ren, Solid State Electron. 41 (1997) 1947.
[17] D.A. Stocker, E.F. Schubert, J.M. Redwing, Appl. Phys. Lett. 73 (1998) 2654.

Contents lists available at ScienceDirect

Physica B

journal homepage: www.elsevier.com/locate/physb

Effects of chemical treatment on barrier height and ideality factors of Au/GaN Schottky diodes

M. Diale *, F.D. Auret

Department of Physics, University of Pretoria, Lynwood Road, Pretoria 0002, South Africa

ARTICLE INFO

PACS:
73.30.+y
79.40.+z

Keywords:
Surface treatment
Schottky contact

ABSTRACT

We have studied Au/*n*-GaN Schottky barrier diodes. GaN surfaces have been prepared by cleaning in HCl and $(NH_4)_2S$ prior to metal deposition. The zero-biased barrier heights and ideality factors obtained from the current–voltage characteristics differ from diode to diode, although all the samples were prepared identically. The statistical analysis for the reverse bias *C–V* data yielded mean value of (1.35 ± 0.04) eV for Schottky barrier height of HCl treated sample and (1.20 ± 0.03) eV for $(NH_4)_2S$ sample, where 9 dots were considered from each cleaning method. It was found that the barrier height values obtained from the C^{-2}–V (1.43 eV) and *I–V* characteristics (0.89 eV) are different from each other by 0.54 eV. The inhomogeneous barrier heights were found to be related to the effect of the high series resistance on diode parameters (Akkiliç et al., 2004) [1].

1. Introduction

Rectifying contacts with low leakage currents and high barrier height are required for the successful fabrication of GaN-based devices. Schottky barrier diodes (SBD) are the choice structure for many semiconductor devices, including microwave diodes, field-effect transistors and photodiodes [2–4]. Their technological importance requires a full understanding of the nature of the electrical characteristics of SBDs. It is well known that SBD has a thin layer of an oxide between the metal and the semiconductor, which cannot be removed by conventional chemical cleaning. Such an oxide converts the diode to metal–insulator–semiconductor (MIS) and usually influences the electrical characteristics of the diode, causing a change in the interfacial charge with bias, giving rise to an electric field at the interfacial layer between the metal and the semiconductor [5,6]. The oxide layer reduces the barrier height and consequently increases the series resistance.

Generally, the forward biased current–voltage (*I–V*) characteristics are linear in the semi-logarithmic scale at low voltages, but deviate considerably from linearity due to the effects of series resistance, R_s resulting from the presence of the thin oxide layer and other surface contaminants. The series resistance is only effective in the curvature downward region or non-linear region of the forward *I–V* characteristics at sufficiently high voltages. The concavity of the current–voltage characteristics at higher voltages increases with increasing series resistance. Increasing series resistance decreases the barrier height and this result in non-ideal current–voltage characteristics. Other parameters such as the ideality factor, $n(V)$ and zero bias barrier height, $\Phi_{b,0}$ are effective in both the linear and the non-linear regions of the *I–V* curve, accompanying the changes in the Schottky barrier height (SBH) [7]. The effect of the series resistance between the depletion region and the ohmic contact of the neutral region of the semiconductor bulk causes the *I–V* characteristics of the metal–semiconductor contact to deviate from the expected [8].

The interface states at the metal–semiconductor junction play a vital role in evaluating the Schottky barrier height and the ideality factor. These manifest themselves as deviations from the ideal Schottky barrier formation and are localized within a few atomic layers of the intimate metal–semiconductor contact with energies which fall inside the forbidden gap. Bardeen showed that such charge accumulated at the metal–semiconductor contact reduces the effective potential difference between the semiconductor and the metal contact [9]. Interface states arise from semiconductor surface states due to discontinuity in the lattice potential, metal-induced-gap states due to wave-function tunneling from the metal into the semiconductor, surface states due to contamination and defects; and any new compounds formed as a result of the interaction of the metal and the semiconductor.

A study of the importance of series resistance in calculating the characteristic parameters of Si Schottky contacts was done by Aydin et al. [1], obtaining their estimations from determination of interface states density distribution from the analysis of the current–voltage measurements. Kampen and Monch studied the barrier heights of different metals on GaN using metal-induced gap states (MIGS) and the electronegativity model, concluding that the experimental values of the barrier height are excellently reproduced by the theoretical predictions, which follow from

* Corresponding author. Tel.: +27 12 420 4418; fax: +27 12 362 5288.
E-mail address: mmantsae.diale@up.ac.za (M. Diale).

0921-4526/$ - see front matter © 2009 Elsevier B.V. All rights reserved.
doi:10.1016/j.physb.2009.09.039

physical MIGS and the electronegativity concept [10]. A review of metal-contact technology has revealed the importance of surface preparation prior to metal deposition [11]. In this study, two different surface chemicals were used to treat GaN surface prior to metal deposition. The effects of chemical treatments on Schottky characteristics were investigated using capacitance–voltage (*C*–*V*) and current–voltage (*I*–*V*) characteristics. The average barrier height for the diodes was 1.43 and 1.20 eV for *C*–*V*; and 0.81 and 0.89 for *I*–*V* measurements, respectively.

2. Experimental

For this investigation, we have used GaN samples with carrier density of $1\times10^{17}\,\text{cm}^{-3}$, obtained from TDI. Before contact fabrication, samples were cleaned using trichloroethylene (TEC), Isopropanol and HCl:HNO_3 aquaregia. Each of these samples was finally etched in 1:1 HCl:H_2O (sample 1) and $(NH_4)_2S$ (sample 2), respectively. Using patterned surface, Ti/Al/Ni/Au (150/2200/400/500 Å) ohmic contacts were deposited by electron-beam and annealed in ultra pure Ar for 5 min at 500 °C. Thereafter, Au Schottky contacts, 0.25 mm thick, were deposited in the resistive evaporator at room temperature. The values of zero-biased barrier height and ideality factor were determined from *I*–*V* and *C*–*V* measurements at room temperature and corrected afterwards for the effect of series resistance.

3. Results and discussion

In Schottky diodes, the depletion layer capacitance can be expressed as [2]

$$C^{-2} = \frac{2(V_{bi} - V_A)}{q\varepsilon_s A^2 N_D} \tag{1}$$

where *A* is the area of the diode, V_{bi} the diffusion potential at zero bias and is determined from the extrapolation of the linear $C^{-2} - V$ plot to the *V* axis and V_A is the applied voltage. The value of the barrier height can be obtained from the relation:

$$\Phi_{b,0}(C-V) = V_{bi} + V_0 \tag{2}$$

where V_0 is the potential difference between the bottom of the conduction band and the Fermi level; and can be calculated knowing the donor concentration N_D obtained from the following relation:

$$V_0 = (kT)\ln\left(\frac{N_C}{N_D}\right) \tag{3}$$

where $N_C = 4.6\times10^{16}\,\text{cm}^{-3}$ is the effective density of states in the conduction band [3].

Nine dots with the same diameter (0.25 mm) on each sample were evaluated. Fig. 1 shows the reverse bias $C^{-2} - V$ characteristics for one diode from sample 1 and sample 2, respectively. For these particular diodes on samples 1 and 2, the *C*–*V* barrier heights are 1.43 and 1.20 eV, respectively. The carrier concentration of 1.9×10^{16} and $2.4\times10^{16}\,\text{cm}^{-3}$ from the reverse bias $C^{-2} - V$ plots was obtained for samples 1 and 2. The *C*–*V* barrier heights ranged from 1.28 to 1.50 eV for sample 1 and from 1.14 to 1.25 eV for sample 2. The statistical analysis for the *C*–*V* data yielded SBH mean value of 1.35 ± 0.04 eV for sample 1 dots and SBH mean value of 1.20 ± 0.03 eV for sample 2.

In Schottky barrier diodes, the barrier height depends on the voltage and surface conditions prior to metal deposition. The surface condition includes the thickness of the interfacial oxide, which affects the current–transport mechanisms. These include the thermionic emission, which is characterized by ideality close to unity and thermionic field emission and field emission. These mechanisms are affected by series resistance, tunneling and generation recombination in the depletion region. Table 1 gives the summary of the electrical characteristics of the diodes.

For a Schottky contact with series resistance, the net current of the device is due to thermionic emission and it is written as [2]

$$I = I_0 \exp\left(-\frac{q(V_A - IR_s)}{nkT}\right) \tag{4}$$

where the saturation current, I_0 is expressed as

$$I_0 = AA^*T^2 \exp\left(-\frac{q\Phi_{b,0}}{kT}\right) \tag{5}$$

where *q* is the electron charge, A^* is the effective Richardson constant and is equal to $26\,\text{A/cm}^2\,\text{K}^2$ for n-type GaN [12], *A* is the

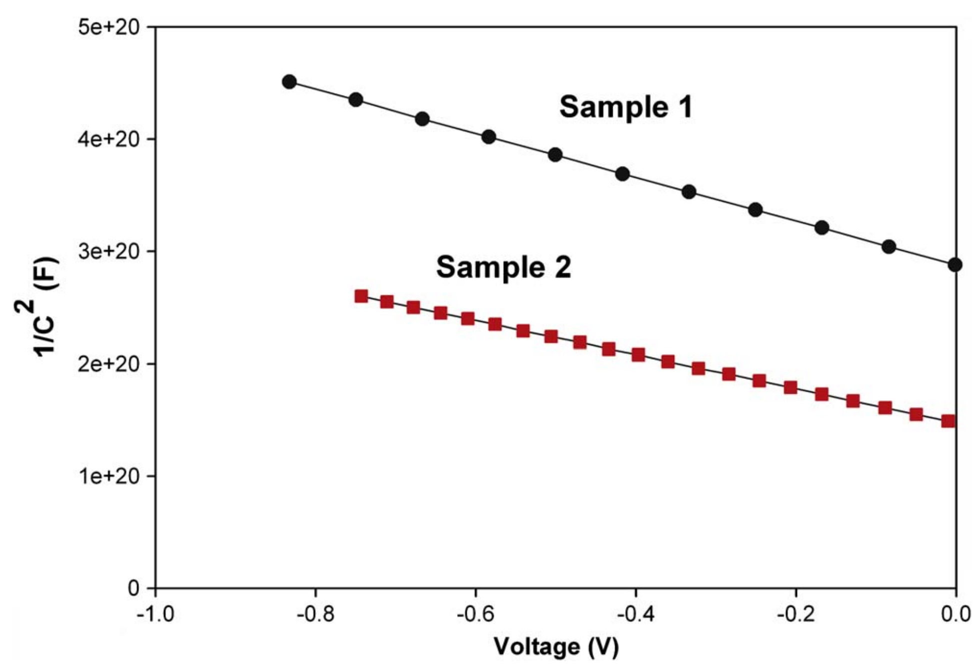

Fig. 1. Reverse bias C^2–*V* curves of the HCl and $(NH_4)_2S$ samples. For these particular diodes on samples 1 and 2, the *C*–*V* barrier heights are 1.43 and 1.20 eV, respectively.

diode area, T is the absolute temperature, k Boltzmann constant, n the ideality factor of the SBD and $\Phi_{b,0}$ the zero bias barrier height. When $V_A \geq 3kT/q$, the extrapolated current, I_0 and the zero bias barrier height can be expressed as

$$\Phi_{b,0} = \frac{kT}{q} \ln\left(\frac{A^* A T^2}{I_0}\right) \tag{6}$$

and the ideality factor from Eq. (4) can be written as

$$n = \frac{q}{kT} \frac{dV}{d(\ln I)} \tag{7}$$

The ideality factor of the SBD, n is a measure of the conformity of the diode to pure thermionic emission. From Fig. 2, current–transport mechanisms displayed are thermionic emission and the series resistance effect at high voltages. The values of the ideality factor, n and the barrier height, Φ_b were calculated from the forward I–V characteristics according to Eqs. (6) and (7). For sample 1 the barrier height, $\Phi_{b,0}$ ranged from 0.79 to 0.89 eV and the ideality factor n ranged from 1.02 to 1.17. Sample 2 $\Phi_{b,0}$ values ranged from 0.71 to 0.85 eV and the n from 1.31 to 1.36. The statistical analysis yielded mean values of 0.84 ± 0.05 eV for the 1.06 ± 0.50 for barrier height and ideality factor of sample 1 (9 dots), respectively, and the mean values of 0.80 ± 0.01 eV and 1.34 ± 0.20 (9 dots) for sample 2 diodes. Ideality factors above unity has been attributed to interface states due to thin oxide layer between the metal and the semiconductor, including other contaminants, tunneling currents in highly doped semiconductors, image-force lowering of the Schottky barrier in electric field at the interface and generation-recombination currents within the depletion region [2]. Our previous results have shown S and Cl residues onto GaN after cleaning in HCl and $(NH_4)_2S$ using Auger electron spectroscopy (AES) and X-ray photoelectron spectroscopy (XPS) [13]. The work done on GaAs and GaP nitridation has shown anion exchange where a thin layer of Ga–N was formed on each of the materials [14]. Surface Ga–N in turn passivates the GaAs and GaP, affecting the I–V and C–V characteristics of these materials. In addition, the work done by Liu et al. has shown that the Ga peak becomes larger when samples are cleaned in $(NH_4)_2S$ than in HF/HCl [15]. Furthermore, $(NH_4)_2S$ has been found to reduce the barrier height on GaN, and preventing re-oxidation of the surface [16]. We suggest that there exist Ga–Cl and Ga–S on sample 1 and sample 2, respectively. Previous XPS results have shown that as-grown GaN surface has oxides in the form of Ga_2O_3 and GaOH. In addition, while rinsing GaN in water, addition of OH to GaN to form the GaOH, may occur, and be part of sticking surface water that may contribute to interface states [17].

The values of R_s and $\Phi_{b,0}$ for both samples 1 and 2 were obtained as 0.82 eV and 22.3 Ω; and 0.71 eV and 17.0 Ω, respectively. As mentioned above, the barrier height values of 1.43 and 1.20 eV for samples 1 and 2 were obtained from the C^{-2}–V plots, respectively. These barrier height values obtained from the C^{-2}–V (1.43 eV) and I–V characteristics (0.89 eV) are different from each other by 0.54 eV. We attribute the difference between the I–V and C–V barrier height in the metal–semiconductor to SBH inhomogeneity. This is the fact that the barrier heights of the diodes on the same sample differs from diode to diode and at different positions on the same diode. The measured I–V barrier height is significantly lower than the weighted arithmetic average of the SBHs. On the other hand, the C–V measured barrier height is influenced by the distribution of charge at the depletion region follows the weighted arithmetic average of the barrier height inhomogeneity; hence the BH determined by C–V is close to the weighted arithmetic average of the barrier heights. Therefore, the

Table 1
Values obtained experimentally from the current–voltage characteristics of the Au/GaN Schottky diodes.

Sample 1	
n	1.17
R_s (Ω)	22.3
$\Phi_{b,c}$ (eV), C–V	1.43
$\Phi_{b,0}$ (eV), I–V	0.82
Sample 2	
n	1.89
R_s (Ω)	17.1
$\Phi_{b,c}$ (eV), C–V	1.20
$\Phi_{b,0}$ (eV), I–V	0.71

The difference in series resistance for the samples 1 and 2 is due to the surface state after different chemical treatment.

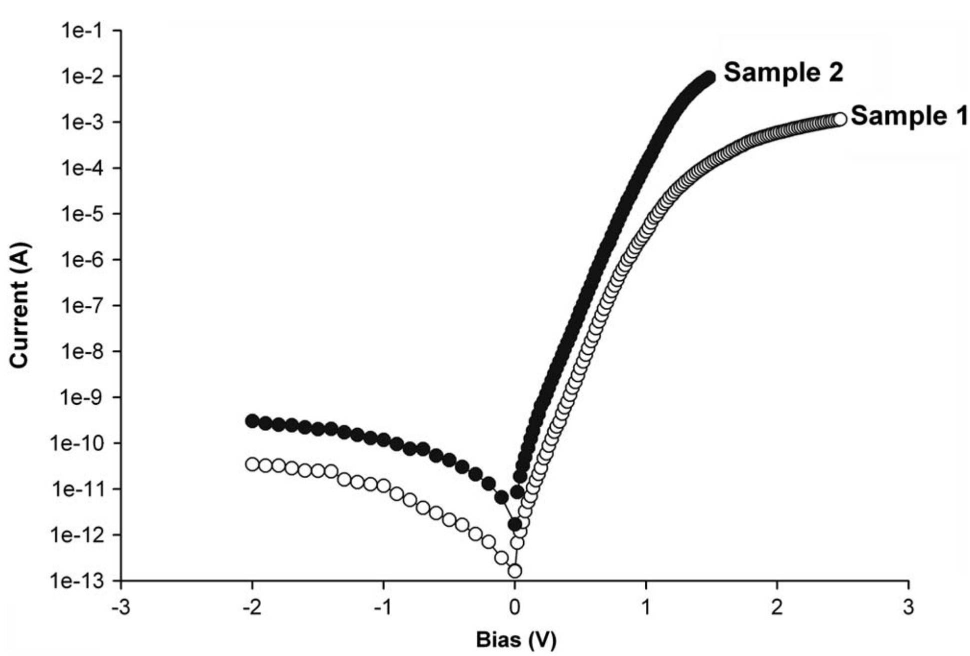

Fig. 2. The I–V curves of the treated samples. The series resistance values of HCl samples are generally higher than those treated in $(NH_4)_2S$, which presented less oxide and reduced barrier height.

barrier height determined from zero bias intercept assuming thermionic emission as current transport mechanism is well below the measured BH and the weighted arithmetic average of the barrier heights [18,19]. Furthermore, the surface damage at the metal–semiconductor interface affects the *I*–*V* measurements because defects may act as recombination centers for trap-assisted tunneling currents. *C*–*V* measurements are generally less prone to interface states, so that the determined barrier height is considered more reliable, though the depletion width can be altered by the interface defects if they are deeper into the space charge region [20].

4. Summary

In conclusion, we have fabricated Au/*n*-GaN SBDs using different cleaning procedures. From the current–voltage characteristics, we obtained the values of ideality factor, SBH and R_s for the samples. The *I*–*V* characteristics are near ideal with thermionic emission as the dominant current transport mechanism. Furthermore, HCl treated samples behave like a MIS diode due to the amount of oxide remaining on the surface after treatment. The series resistance values of HCl samples are generally higher than those treated in $(NH_4)_2S$, which presented less oxide and reduced barrier height, in agreement with published results. Most published results on GaN have only reported their findings without specifics on current transport mechanism. Thus further work is needed for the investigation ideality factor far above unity, which will need the knowledge of the oxide layer thickness on GaN, effects of passivation of GaN surface on electrical characteristics, and analysis of barrier height inhomogeneities on the rectifying diode characteristics on GaN.

Acknowledgment

The authors gratefully acknowledge financial assistance from the South African National Research Foundation.

References

[1] K. Akkiliç, M.E. Aydin, A. Türüt, Physica Scripta 70 (2004) 364.
[2] E.H. Rhoderick, R.H. Williams, Metal–Semiconductor Contacts, Clarendon Press, Oxford, 1988.
[3] S.M. Sze, Physics of Semiconductor Devices, second ed., Wiley, New York, 1981.
[4] L. Wang, M.I. Nathan, T.-H. Lim, M.A. Khan, Q. Chen, Applied Physics Letters 68 (9) (1996) 1267.
[5] P. Hanselaer, W.H. Laflere, R.L. Meirhaeghe, F. Cardon, Applied Physics Letters 56 (1984) 2309.
[6] E. Monroy, F. Calle, J.L. Pau, E. Muńoz, F. Omnes, Electronic Letters 36 (25) (2000) 2096.
[7] J.C. Card, E.H. Rhoderick, Journal of Applied Physics D 4 (1971) 1589.
[8] M.E. Aydin, K. Akkiliç, T. Kiliçoglu, Applied Surface Science 225 (2004) 1304.
[9] J. Bardeen, Physical Review 71 (1947) 771.
[10] T.U. Kampen, W. Monch, Applied Surface Science 117/118 (1997) 388.
[11] Q.Z. Liu, S.S. Lau, Solid State Electronics 42 (1998) 677.
[12] A.C. Schmidt, A.T. Ping, M. Asif Khan, Q. Chen, J.W. Yang, I. Adesida, Semiconductor Science and Technology 11 (1996) 1464.
[13] M. Diale, F.D. Auret, N.G. van der Berg, R.Q. Odendaal, W.D. Roos, Applied Surface Science 246 (2005) 279.
[14] G. Bruno, Applied Surface Science 235 (2004) 239.
[15] J. Liu, B. Shen, Y.G. Zhou, H.M. Zhou, M.J. Wang, Z.W. Zheng, B. Zhang, Y. Shi, Y.D. Zheng, Optical Materials 23 (2003) 133.
[16] X.A. Cao, S.J. Pearton, G. Dang, A.P. Zhang, F. Ren, J.M. Van Hove, Applied Physics Letters 75 (1999) 4130.
[17] M. Diale, F.D. Auret, N.G. van der Berg, R.Q. Odendaal, W.D. Roos, Surface and Interface Analysis 37 (2005) 1158.
[18] J.H. Werner, H.H. Guttler, Journal of Applied Physics 69 (3) (1991) 1552.
[19] R.T. Tung, A.F.J. Levi, J.P. Sullivan, F. Schrey, Physical Review Letters 66 (1) (1971) 72.
[20] C. Fontaine, T. Okumura, K.N. Tu, Journal of Applied Physics 54 (1983) 1404.